Journal of Sound and Vibration (2000) **238**(3), 425–441
doi:10.1006/jsvi.2000.3086, available online at http://www.idealibrary.com on IDEAL®

SOUND RADIATION FROM A FINITE FLUID-FILLED/SUBMERGED CYLINDRICAL SHELL WITH POROUS MATERIAL SANDWICH

C. J. Wu, H. L. Chen and X. Q. Huang

Institute of Vibration and Noise Control, School of Mechanical Engineering, Xi'an Jiaotong University, Xi'an, Shaanxi 710049, *The People's Republic of China*

(*Received* 28 *October* 1999, *and in final form* 12 *May* 2000)

A theoretical model is developed to predict the far field sound radiation from a finite fluid-filled/submerged cylindrical thin shell with porous material sandwich. A combination of the wave-number domain approach and the transfer matrix method is presented, which is convenient to analyze the vibratory responses in terms of wave number. Expressions for the spectral radial velocity of the outer surface of the shell are also formulated. A prediction model for sound radiation at far field is given by using the boundary integral equation. Extensive numerical results are also presented to illustrate the general characteristics of the far field sound pressure as a function of frequency. An experimental verification is performed, and a good correlation between the theoretical results and the experimental results shows that the theoretical study work in this paper is correct.

1. INTRODUCTION

Porous absorptive materials (e.g. glass wool) offer the noise-control engineers the possibility of designing strong lightweight sandwich structures to reduce the sound radiation from the original single cylindrical shell. In the first stages of design, it is desirable to carry out parametric studies by using the computer programmes based on the theoretical models. An impedance model for analyzing acoustic characteristics of lagged pipes has been given by Munjal [1], who used the transfer matrix method to predict the transverse insertion loss. In addition, Skelton and James [2] have studied the acoustics of anisotropic-layered cylinder by using a combination of the wave-number domain approach and the finite element method. However, their studies are only focused on an infinite cylindrical sandwich shell. To the author's knowledge, little work has been done to investigate the sound radiation characteristics of a finite fluid-filled/submerged cylindrical shell with porous material sandwich. This kind of problem, which belongs to multi-layer fluid-structure couplings, is in general significantly more complex than the corresponding problem with a shell of infinite length. Until now, other than the method addressed in reference [1], or the methods given in references [2–8], few effective methods have been used to solve such a problem successfully. This is the aim of this paper.

This paper consists of both theoretical investigation and experimental verification on the far field sound radiation from a finite fluid-filled/submerged cylindrical thin elastic shell with porous material sandwich. Section 2 of this paper details the theory: a theoretical model of vibration analysis for this kind of fluid-filled/submerged shell is developed by using a combination of the wave number domain approach (cf. references [2–4]) and the

0022-460X/00/480425 + 17 $35.00/0

transfer matrix method (cf. reference [1]). Accordingly, an expression for the spectral radial velocity of the outer surface of the shell is presented. Section 3 presents a prediction model for the far field sound pressure by using the boundary integral equation (cf. reference [9]), which involves the spectral radial velocity addressed in section 2. In section 4, extensive numerical results are also presented to illustrate general characteristics of the far field sound pressure as a function of frequency. Section 5 describes the experimental set-up and compares the theoretical model predictions with measured results. Finally, section 6 concludes on the main phenomena that emerge from the theoretical model and experiments, and summarizes the criteria that predict the far field sound radiation from this kind of shell.

This study has three main originalities. First, it quantifies for the first time the far field sound radiation from a finite fluid-filled/submerged cylindrical sandwich shell under a radial harmonic point load. Second, it uses a combination of the wave number domain approach and the transfer matrix method to analyze the vibration responses and to present an expression for the spectral radial velocity of the outer surface of this kind of shell. Finally, it gives an experimental validation of the theoretical model for such a system.

2. BASIC THEORY

2.1. STATEMENT OF THE PROBLEM

Consider a finite fluid-filled/submerged cylindrical sandwich shell, which is shown in Figure 1, where a cylindrical co-ordinates system (r, φ, z) is used to define the position of points on the shell surface or in the fluids. Note that the shell consists of three parts: The

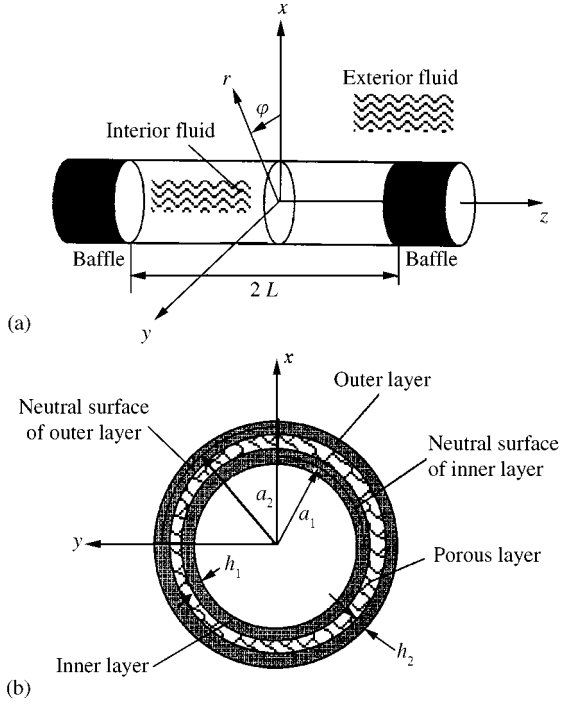

Figure 1. Fluid-filled/submerged cylindrical sandwich shell and co-ordinate system.

inner layer, the outer layer and the porous material layer. The shell is terminated by two semi-infinite cylindrical rigid baffles and is excited by an internal or external harmonic point load. Both the exterior fluid and the interior fluid are assumed to be stationary and non-viscous. It is also assumed that there is no other energy source in the fluids. So structural-acoustic couplings exist among the interior fluid, the inner layer, the porous material layer, the outer layer and the exterior fluid. This kind of multi-layer coupling problem can be solved by the transfer matrix equations of aforementioned three layers in the wave-number domains, and by the boundary integral equation.

In the subsequent sections, a list of symbols is given in Appendix B, and the time-variation factor $e^{-j\omega t}$ is suppressed for the sake of brevity.

2.2. VIBRATION ANALYSIS

2.2.1. *Transfer matrix equations of the inner layer and the outer layer in the wave-number domain*

First, we will consider the inner layer in terms of the classical assumption of Donnell. By using Fourier integral transform in the z direction and Fourier series transform in the φ direction, one can get the inner layer equation of motion in the wave-number domain as follows:

$$\begin{bmatrix} \tilde{u}_{z,n}(a_1,\zeta) \\ \tilde{u}_{\varphi,n}(a_1,\zeta) \\ \tilde{u}_{r,n}(a_1,\zeta) \end{bmatrix} = \frac{1-\nu_1^2}{E_1 h_1}[\tilde{\Gamma}_{1n}] \begin{bmatrix} -\tilde{S}^+_{z,n}(a_1,\zeta) + \tilde{S}^-_{z,n}(a_1,\zeta) \\ -\tilde{S}^+_{\varphi,n}(a_1,\zeta) + \tilde{S}^-_{\varphi,n}(a_1,\zeta) \\ [\tilde{F}_{r,n}(r_i,\zeta) + \tilde{p}_n(r_i,\zeta) - \tilde{p}_n(r_1,\zeta)] - \tilde{S}^+_{r,n}(a_1,\zeta) + \tilde{S}^-_{r,n}(a_1,\zeta) \end{bmatrix}, \tag{1}$$

where the spectral variables are given by Skelton and James [2]

$$\tilde{f}_n(r,\zeta) = \int_{-\infty}^{\infty} f_n(r,z)\, e^{-jz\zeta}\, dz \quad \text{and} \quad f_n(r,z) = \frac{1}{2\pi}\int_0^{2\pi} f(r,\varphi,z)\, e^{-jn\varphi}\, d\varphi. \tag{2a,b}$$

According to equation (1), the spectral radial displacement of the neutral surface of the inner layer is easily obtained as (cf. references [10, 11])

$$\tilde{u}_{r,n}(a_1,\zeta) = \frac{1-\nu_1^2}{E_1 h_1}\tilde{\Gamma}^3_{n3}(a_1,\zeta)\{\tilde{X}_n(a_1,\zeta) + [\tilde{F}_{r,n}(r_i,\zeta) + \tilde{p}_n(r_i,\zeta) - \tilde{p}_n(r_1,\zeta)]\}, \tag{3}$$

where

$$\begin{aligned} \tilde{X}_n(a_1,\zeta) = \frac{1}{\tilde{\Gamma}^3_{n3}(a_1,\zeta)} \{ & \tilde{\Gamma}^1_{n3}(a_1,\zeta)[-\tilde{S}^+_{z,n}(a_1,\zeta) + \tilde{S}^-_{z,n}(a_1,\zeta)] \\ & + \tilde{\Gamma}^2_{n3}(a_1,\zeta)[-\tilde{S}^+_{\varphi,n}(a_1,\zeta) + \tilde{S}^-_{\varphi,n}(a_1,\zeta)] \\ & + \tilde{\Gamma}^3_{n3}(a_1,\zeta)[-\tilde{S}^+_{r,n}(a_1,\zeta) + \tilde{S}^-_{r,n}(a_1,\zeta)]\}. \end{aligned} \tag{4}$$

Accordingly, the spectral radial velocity of the neutral surface of the inner layer is

$$\tilde{\dot{u}}_{r,n}(a_1,\zeta) = -j\omega\tilde{u}_{r,n}(a_1,\zeta) = -j\omega\frac{1-v_1^2}{Eh_1}\tilde{\Gamma}^3_{n3}(a_1,\zeta)$$

$$\times\{\tilde{X}_n(a_1,\zeta)+[\tilde{F}_{r,n}(r_i,\zeta)+\tilde{p}_n(r_i,\zeta)-\tilde{p}_n(r_1,\zeta)]\}. \tag{5}$$

Moreover, the spectral radial velocities among the inner surface, the neutral surface and the outer surface of the thin inner layer are identical i.e.,

$$\tilde{\dot{u}}_{r,n}(r_i,\zeta)=\tilde{\dot{u}}_{r,n}(r_1,\zeta)=\tilde{\dot{u}}_{r,n}(a_1,\zeta). \tag{6}$$

By combining equation (5) with equation (6), one can write the transfer matrix equation of the inner layer in the wave-number domain as follows:

$$\begin{bmatrix}\tilde{p}_n(r_i,\zeta)+\tilde{F}_{r,n}(r_i,\zeta)+\tilde{X}_n(a_1,\zeta)\\ \tilde{\dot{u}}_{r,n}(r_i,\zeta)\end{bmatrix}=\begin{bmatrix}1 & \tilde{Z}_{1,n}(a_1,\zeta)\\ 0 & 1\end{bmatrix}\begin{bmatrix}\tilde{p}_n(r_1,\zeta)\\ \tilde{\dot{u}}_{r,n}(r_1,\zeta)\end{bmatrix}, \tag{7}$$

where

$$\tilde{Z}_{1,n}(a_1,\zeta) = -\frac{E_1h_1}{\mathrm{j}\omega(1-v_1^2)\tilde{\Gamma}^3_{n3}(a_1,\zeta)}. \tag{8}$$

It is noted that equation (7) involves the spectral variables (pressure $\tilde{p}_n(r,\zeta)$ and radial velocity $\tilde{\dot{u}}_{r,n}(r,\zeta)$) on the inner surface of the inner layer related to those on the outer surface of the inner layer.

Similarly, the transfer matrix equation of the outer layer in the wave-number domain can be easily obtained as follows:

$$\begin{bmatrix}\tilde{p}_n(r_2,\zeta)\\ \tilde{\dot{u}}_{r,n}(r_2,\zeta)\end{bmatrix}=\begin{bmatrix}1 & \tilde{Z}_{2,n}(a_2,\zeta)\\ 0 & 1\end{bmatrix}\begin{bmatrix}\tilde{p}_n(r_o,\zeta)+\tilde{F}_{r,n}(r_o,\zeta)-\tilde{X}_n(a_2,\zeta)\\ \tilde{\dot{u}}_{r,n}(r_o,\zeta)\end{bmatrix}. \tag{9}$$

Here all the spectral variables have the same meanings as for those of the inner layer.

2.2.2. *Transfer matrix equation of porous material layer in the wave-number domain*

According to the general spectral solution of the Helmholtz equation in fluid and the corresponding boundary conditions (cf. reference [2]) at fluid-structure surface, one can get the transfer matrix equation of the porous material layer in the wave-number domain as

$$\begin{bmatrix}\tilde{p}_n(r_1,\zeta)\\ \tilde{\dot{u}}_{r,n}(r_1,\zeta)\end{bmatrix}=[\mathbf{T}_m]\begin{bmatrix}\tilde{p}_n(r_2,\zeta)\\ \tilde{\dot{u}}_{r,n}(r_2,\zeta)\end{bmatrix}, \tag{10}$$

where the spectral transfer matrix $[\mathbf{T}_m]$ is

$$[\mathbf{T}_m]=\begin{bmatrix}T^m_{11} & T^m_{12}\\ T^m_{21} & T^m_{22}\end{bmatrix}=\frac{1}{D}\begin{bmatrix}Q(J_{n,1}H'_{n,2}-J'_{n,2}H_{n,1}) & J_{n,2}H_{n,1}-J_{n,1}H_{n,2}\\ Q^2(J'_{n,1}H'_{n,2}-J'_{n,2}H'_{n,1}) & Q(J_{n,2}H'_{n,1}-J'_{n,1}H_{n,2})\end{bmatrix}, \tag{11}$$

here

$$Q \equiv \frac{\gamma_m}{\mathrm{j}k_m Y_m}, \tag{12}$$

$$D \equiv Q(J_{n,2}H'_{n,2} - J'_{n,2}H_{n,2}), \tag{13}$$

$$J_{n,1} \equiv \mathrm{J}_n(\gamma_m r_1), \quad J'_{n,1} \equiv \mathrm{J}'_n(\gamma_m r_1), \quad H_{n,1} \equiv \mathrm{H}_n(\gamma_m r_1), \quad H'_{n,1} \equiv \mathrm{H}'_n(\gamma_m r_1), \quad \text{etc.} \tag{14a–d}$$

For commercially available mineral wool and glass wool, the wave number k_m and the characteristic impedance Y_m are given in reference [1]. Recently, a new absorptive porous material known as metal fibre has been widely used in many industrial fields. This kind of engineering material is made up of many stainless-steel ribbons, and has an advantage over the common porous materials in high strength and corrosion-resistance. Based on a number of experimental results, expressions for the wave number and the characteristic impedance of the metal fibre are given by using the genetic algorithm as follows [11]:

$$Y_m = Y_f(0{\cdot}7996 f^{-0{\cdot}1887}\rho_m^{0{\cdot}2903} - \mathrm{j}0{\cdot}0314 f^{-0{\cdot}8396}\rho_m^{1{\cdot}2458}), \tag{15}$$

$$k_m = k_f(1{\cdot}8574 f^{-0{\cdot}1399}\rho_m^{0{\cdot}1035} - \mathrm{j}0{\cdot}0596 f^{-0{\cdot}7507}\rho_m^{1{\cdot}2356}). \tag{16}$$

2.2.3. *The shell responses*

After combining equations (7), (10), (11) with (9), it can be shown that

$$\begin{bmatrix} \tilde{p}_n(r_i,\zeta) + \tilde{F}_{r,n}(r_i,\zeta) + \tilde{X}_n(a_1,\zeta) \\ \tilde{\tilde{u}}_{r,n}(r_i,\zeta) \end{bmatrix} = \begin{bmatrix} 1 & \tilde{Z}_{1,n}(a_1,\zeta) \\ 0 & 1 \end{bmatrix} \begin{bmatrix} T^m_{11} & T^m_{12} \\ T^m_{21} & T^m_{22} \end{bmatrix} \begin{bmatrix} 1 & \tilde{Z}_{2,n}(a_2,\zeta) \\ 0 & 1 \end{bmatrix} \times \begin{bmatrix} \tilde{p}_n(r_o,\zeta) + \tilde{F}_{r,n}(r_o,\zeta) - \tilde{X}_n(a_2,\zeta) \\ \tilde{\tilde{u}}_{r,n}(r_o,\zeta) \end{bmatrix}. \tag{17}$$

The solution to equation (17) is

$$\tilde{\tilde{u}}_{r,n}(r_0,\zeta) = \frac{-[\tilde{F}_{r,n}(r_i,\zeta) + \tilde{X}_n(a_1,\zeta)] - [\tilde{F}_{r,n}(r_o,\zeta) - \tilde{X}_n(a_2,\zeta)]\{T^m_{21}[\tilde{Z}_{i,n}(r_i,\zeta) - \tilde{Z}_{1,n}(a_1,\zeta)] - T^m_{11}\}}{[\tilde{Z}_{o,n}(r_o,\zeta) + \tilde{Z}_{2,n}(a_2,\zeta)]\{T^m_{21}[\tilde{Z}_{i,n}(r_i,\zeta) - \tilde{Z}_{1,n}(a_1,\zeta)] - T^m_{11}\} - T^m_{12} + T^m_{22}[\tilde{Z}_{i,n}(r_i,\zeta) - \tilde{Z}_{1,n}(a_1,\zeta)]}. \tag{18}$$

where $\tilde{Z}_{i,n}(r_i,\zeta)$ and $\tilde{Z}_{0,n}(r_0,\zeta)$ are given by

$$\tilde{Z}_{i,n}(r_i,\zeta) = \frac{\tilde{p}_n(r_i,\zeta)}{\tilde{\tilde{u}}_{r,n}(r_i,\zeta)} = \mathrm{j}\omega\rho_i \frac{\mathrm{J}_n(\gamma_i r_i)}{\gamma_i \mathrm{J}'_n(\gamma_i r_i)}, \tag{19}$$

$$\tilde{Z}_{o,n}(r_o,\zeta) = \frac{\tilde{p}_n(r_o,\zeta)}{\tilde{\tilde{u}}_{r,n}(r_o,\zeta)} = \mathrm{j}\omega\rho_o \frac{\mathrm{H}_n(\gamma_o r_o)}{\gamma_o \mathrm{H}'_n(\gamma_o r_o)}. \tag{20}$$

For the case of external excitation, that is to say, the shell is excited by a radial point load at a point (r_o, φ_o, z_o) on the outer surface of the shell. According to equation (2), the

expression for the spectral exciting force is given by

$$\tilde{F}_{r,n}(r_o, \zeta) = \frac{1}{2\pi} \int_0^{2\pi} \mathrm{e}^{-\mathrm{j}n\varphi} \int_{-\infty}^{+\infty} \frac{F_0}{r_o} \delta(z - z_o)\delta(\varphi - \varphi_o)\mathrm{e}^{-\mathrm{j}z\zeta}\,\mathrm{d}z\,\mathrm{d}\varphi = \frac{F_0}{2\pi r_o}\mathrm{e}^{-\mathrm{j}n\varphi_0 - \mathrm{j}z_o\zeta}. \tag{21}$$

For the case of internal excitation (the shell is excited by a radial point load at a point (r_i, φ_i, z_i) on the inner surface of the shell), similar expression applies for $\tilde{F}_{r,n}(r_i, \zeta)$, where the function is evaluated at (r_i, φ_i, z_i) instead of (r_o, φ_o, z_o).

While substituting equations (4), (8) and (19)–(21) with equation (18), it is shown that the spectral radial velocity of the outer surface of the finite fluid-filled/submerged sandwich shell can be calculated numerically.

3. SOUND PRESSURE AT FAR FIELD

In section 2, the expression for the spectral radial velocity of the outer surface of a finite fluid-filled/submerged cylindrical shell is presented. Here, our main interest is the prediction of the sound radiation at far field. Let M and N be the source point (on the outer surface of the shell) and the observation point (in the exterior fluid), respectively, then the farfield sound pressure can be readily written as (see Appendix A)

$$p(R, \theta, \psi) = \frac{\omega\rho_o \mathrm{e}^{\mathrm{j}k_o R}}{\pi R k_o \sin\theta} \sum_{n=\infty}^{+\infty} \frac{\tilde{u}_{r,n}(r_o, k_o\cos\theta)}{\mathrm{H}_n'(k_o r_o \sin\theta)} \mathrm{e}^{\mathrm{j}n(\psi - \pi/2)}, \tag{22}$$

where $\tilde{u}_{r,n}(r_o, k_o\cos\theta)$ is given by equation (18), in which $\zeta = k_o\cos\theta$.

Note that the far field sound pressure can be easily evaluated when the spectral radial velocity $\tilde{u}_{r,n}(r_o, k_o\cos\theta)$ is known.

Accordingly, the far field sound pressure level is given by

$$L_p = 20\lg\left(\frac{p(R, \theta, \psi)}{p_{ref}}\right), \tag{23}$$

where $p_{ref} = 2 \times 10^{-5}$ Pa.

4. NUMERICAL RESULTS

In this section, the previous theoretical model (see equations (22) and (23)) is used to predict the farfield sound radiation spectra for a simply supported fluid-filled/submerged sandwich shell, containing as excitation a radial point load applied to the inner surface or the outer surface. The shell is supposed to be filled with water and air, and be immersed in water and air. The porous material is selected as the metal fibre. Parameters for the numerical studies are listed in Table 1.

Especially, a single fluid-filled/submerged shell (without porous sandwich) is also considered here, of which the thickness is equal to the sum of all layers of the sandwich shell, and other parameters are all just the same to those of the sandwich shell.

Here, it is of interest to focus our attention to the following four fluid cases for the shell being filled with air and immersed in air; being filled with water and immersed in air; being filled with air and immersed in water; being filled with water and immersed in water.

TABLE 1

Data for the studied shells

	Simulation shell	Experimental shell
Density (kg/m^3)	$\rho_1 = \rho_2 = 7850$, $\rho_m = 270$	$\rho_1 = \rho_2 = 7850$, $\rho_m = 270$
Young's modulus (GN/m^2)	$E_1 = E_2 = 210$	$E_1 = E_2 = 210$
Poisson ratio	$\nu_1 = \nu_2 = 0{\cdot}3$	$\nu_1 = \nu_2 = 0{\cdot}3$
Structural loss factor	$\eta_1 = \eta_2 = 0{\cdot}01$	$\eta_1 = \eta_2 = 0{\cdot}01$
Length (mm)	$L = 190$	$L = 175$
Neutral radius (mm)	$a_1 = 53{\cdot}75$, $a_2 = 56{\cdot}25$	$a_1 = 51{\cdot}25$, $a_2 = 53{\cdot}75$
Thickness (mm)	$h_1 = h_2 = 1{\cdot}5$	$h_1 = h_2 = 1{\cdot}5$
Radial point load (N)	$F_o = 10$	$F_o = 1$
Force location	$z_o = 0$, $\varphi_0 = 0^\circ$	$z_0 = 0$. $\varphi_0 = 180^\circ$
Observation location	$R = 1500$ mm, $\theta = 90^\circ$, $\psi = 0^\circ$	$R = 1500$ mm, $\theta = 90^\circ$, $\psi = 0^\circ$

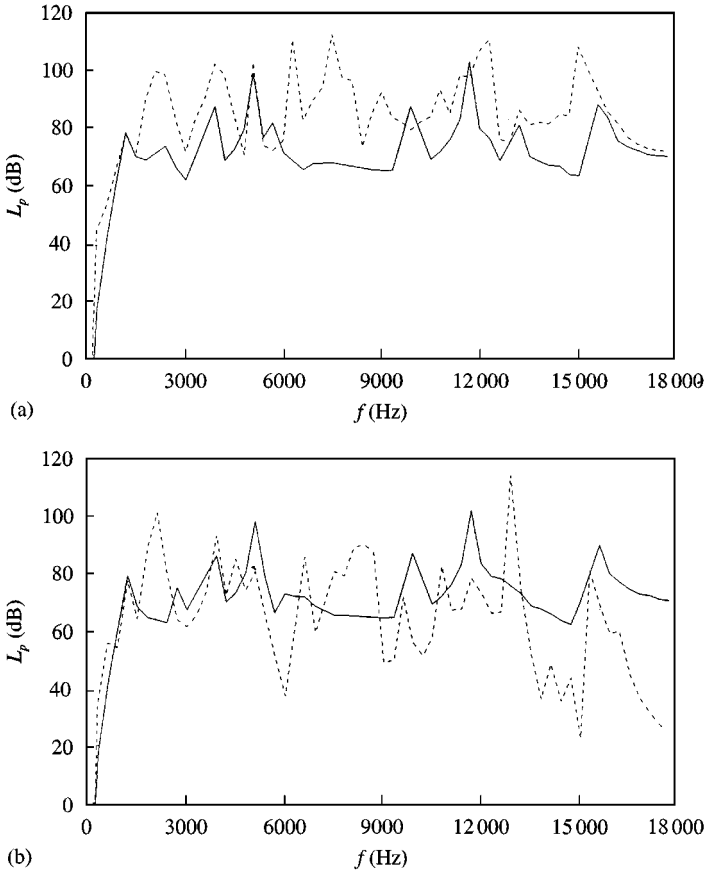

Figure 2. Far field sound radiation spectra of two different shells for the case of being filled with air and immersed in air: (a) External excitation only; (b) internal excitation only; ——, single shell; - - - -, sandwich shell.

Figures 2–5 show respectively, the far field sound radiation spectra comparison between the simulation sandwich shell and the single shell under the external excitation only and the internal excitation only, for all aforementioned four fluid cases. It is of interest to note that for all four fluid cases, the far field sound pressures of the sandwich shell under the internal

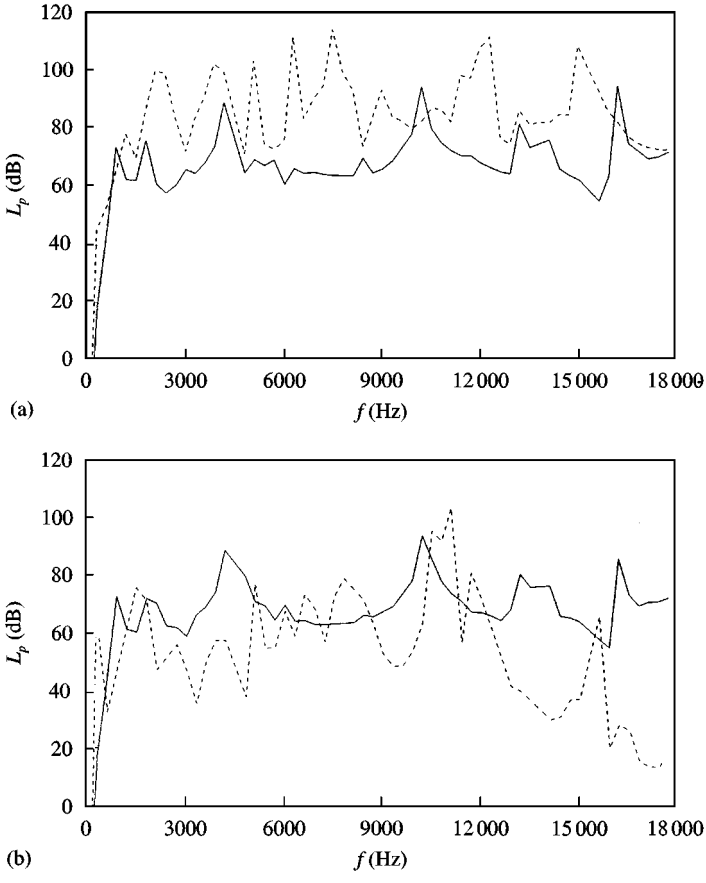

Figure 3. Similar to Figure 2, but the shells are filled with water and are immersed in air (a) and (b); ——, single shell; - - - -, sandwich shell.

excitation are obviously lower than those of the single shell under the same excitation, with the frequency increasing. However, this is not the case of the external excitation for which an opposite situation occurs: the far field sound pressures of the sandwich shell are bigger than those of the single shell for all four fluid cases. To explain this, it is necessary to analyze the structural-acoustic coupling problems between the structures and the fluids in terms of vibratory power transmission. For the case of internal excitation (that is to say, the point load is applied to the internal surface of the inner layer), the vibratory power generated by the inner layer can hardly transmit to the outer layer, as a result of weak coupling existing between the porous material layer (of which the pores are occupied by air) and the two elastic layers (the inner layer and the outer layer). Consequently, the far field sound radiation from the outer layer of the sandwich shell is weak with respect to the case of the single shell. However, for the case of external excitation (that is to say, the point load is applied to the external surface of the outer layer), strong vibratory powers of the outer shell are obtained because of the direct excitation and the same weak coupling cases discussed above. Furthermore, in this case, the thickness of the outer layer is smaller than that of the single shell, thus the far field sound pressures of the outer layer are bigger than those of the single shell.

In addition, it is also noted that when the exterior fluid is fixed, whether the interior fluid is air or water, they both have little influence on the far field sound pressures of the

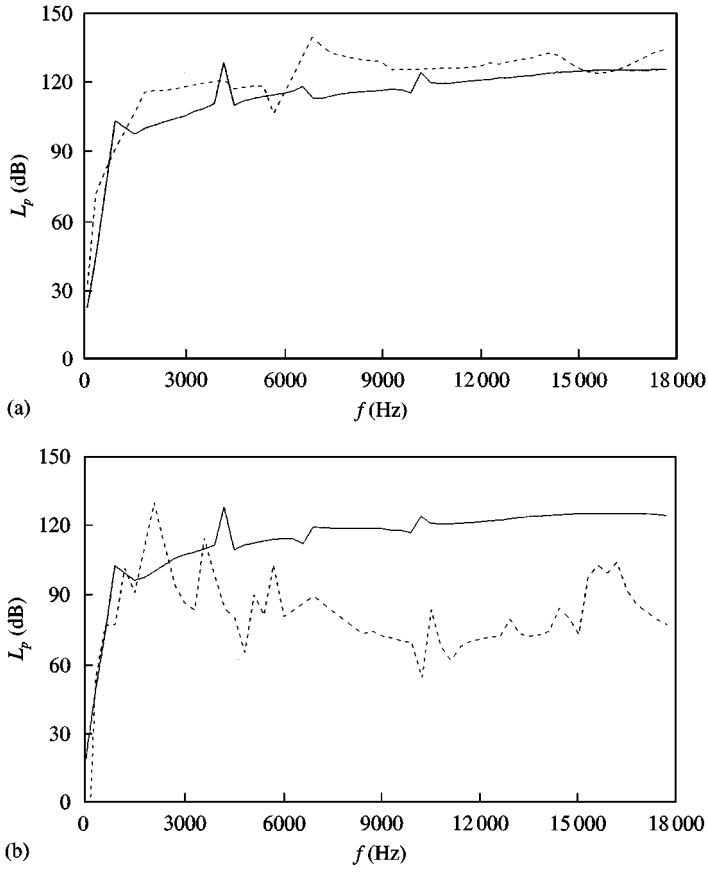

Figure 4. Similar to Figure 2, but the shells are filled with air and are immersed in water (a) and (b); ——, single shell; - - - -, sandwich shell.

sandwich shell. A similar conclusion can be found in reference [11]. On the other hand, when the interior fluid is fixed, the far field sound pressures of the shells (both the sandwich shell and the single shell) immersed in air are very different from those of the shells immersed in water.

Figure 6 shows the far field sound radiation spectra of the sandwich shells with two different porous material layers for the case of being filled with air and immersed in air, and under two cases of excitation. Figure 7 is similar to Figure 6, but the shells are filled with water and are immersed in water. It is noted that the far field sound pressures of the sandwich shell with metal fibre layer are just the same to that of the one with glass wool layer for two fluid cases and two excitation cases. That is to say, metal fibre has better acoustic properties available in industry as well as glass wool.

5. EXPERIMENTAL VERIFICATION

The objective of the experiment is to verify the theoretical model developed above. To this end, an experimental model of simply supported fluid-filled/submerged cylindrical shell is set and the far field sound pressures are measured in an anechoic chamber. A sketch of the

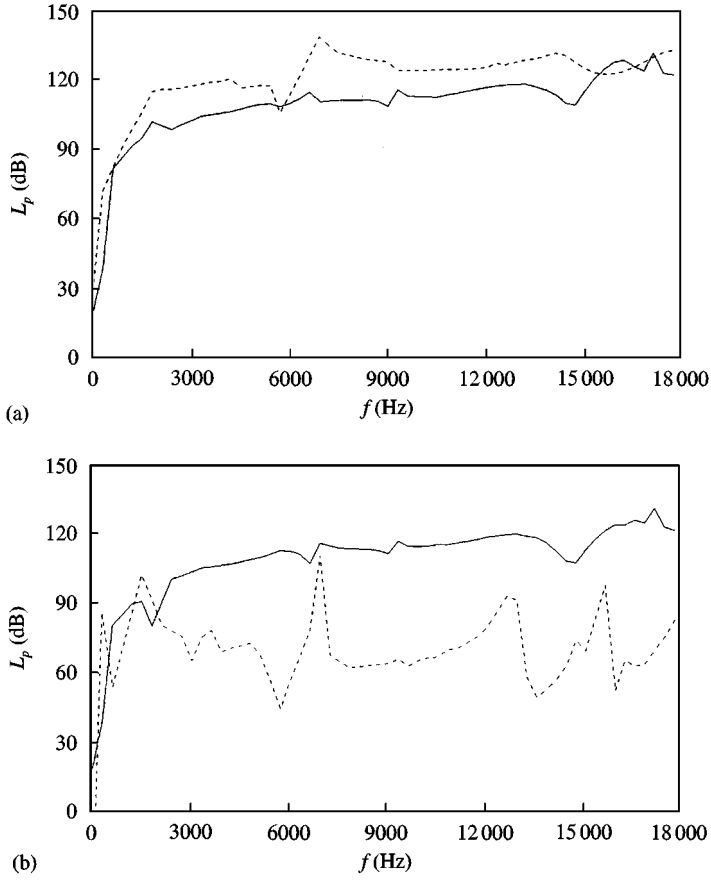

Figure 5. Similar to Figure 2, but the shells are filled with water and are immersed in water (a) and (b); ——, single shell; - - - -, sandwich shell.

measurement system is depicted in Figure 8. The specifications for the experimental shell are given in Table 1, and the shell is supposed to be filled with air or water and immersed in air. The shell consists of two thin steel shells and a metal fibre layer, which is made by using a special assembly method. To approximate the simply supported boundary conditions, two thin discs are welded at both ends of the shell. The shell with the discs is supported on two V-type supporters mounted on a concrete base.

Figure 9 shows the far field sound radiation spectra comparison between the theoretical model and the experimental measurement for the experimental sandwich shell for the case of being filled with air and immersed in air, and under two case of excitation. Figure 10 is similar to Figure 9, but the shell is filled with water and is immersed in air, and under the external excitation only (the internal excitation case is not included here as a result of experimental condition, nevertheless, this has little effect on this experimental verification). It is noted that the differences between the theoretical and experimental results vary approximately from 3 to 10 dB (which are acceptable for applications in the industry), except for several frequencies below 630 Hz for which deviations of over 10 dB are observed. These deviations are likely to be attributed to the three following aspects: the imperfections of the experimental boundary conditions, the inevitable errors of the measurement system, and the simplifications during theoretical modelling process. The first comparison shows

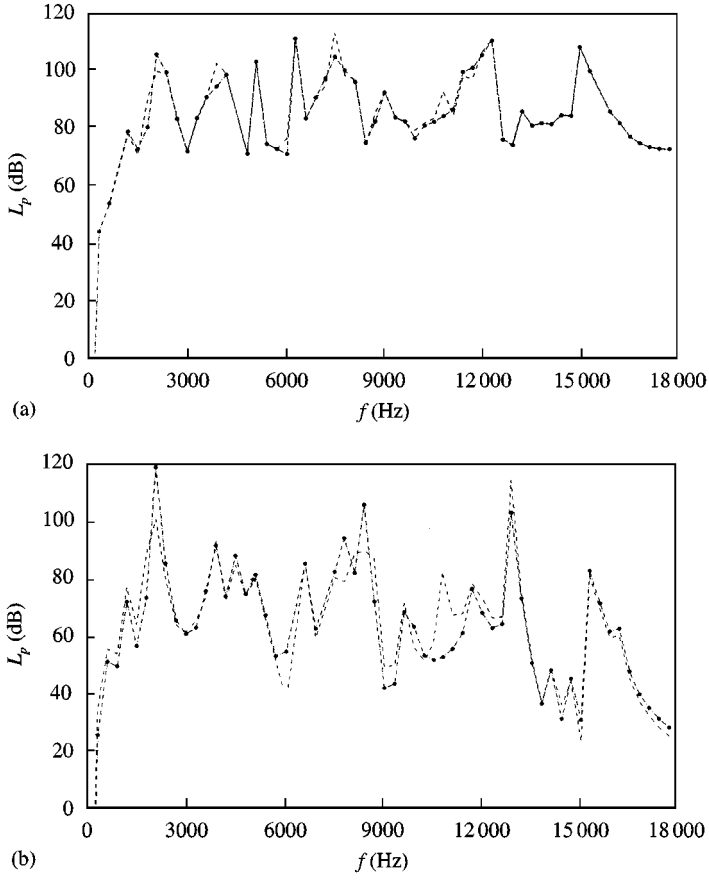

Figure 6. Far field sound radiation spectra of sandwich shells with two different porous layers for the case of being filled with air and immersed in air. (a) External excitation only; (b) internal excitation only; - - - -, metal fibre; -—●—-, glass wool.

that the theoretical model correctly evaluates the far field sound radiation. Furthermore, it is necessary to improve the experimental environment and to amend the theoretical model in the future.

6. CONCLUSIONS

In this paper, a theoretical model has been developed to predict the sound radiation from a finite fluid-filled/submerged cylindrical sandwich shell excited by a radial harmonic point load. The model is based on a combination of the wave-number domain approach, the transfer matrix method and the boundary integral equation, which is convenient to analyze the multi-layer structural-acoustic coupling problem for such a shell in terms of wave number. Extensive numerical studies have been shown that the sandwich shell is very effective to reduce the far field sound radiation from the original single shell for the case of internal excitation. In addition, it is shown that the exterior fluid has great influence on the far field sound radiation from the sandwich shell, contrary to the case of interior fluid. It is also shown that metal fibre has better acoustic properties available in industry as well as glass wool.

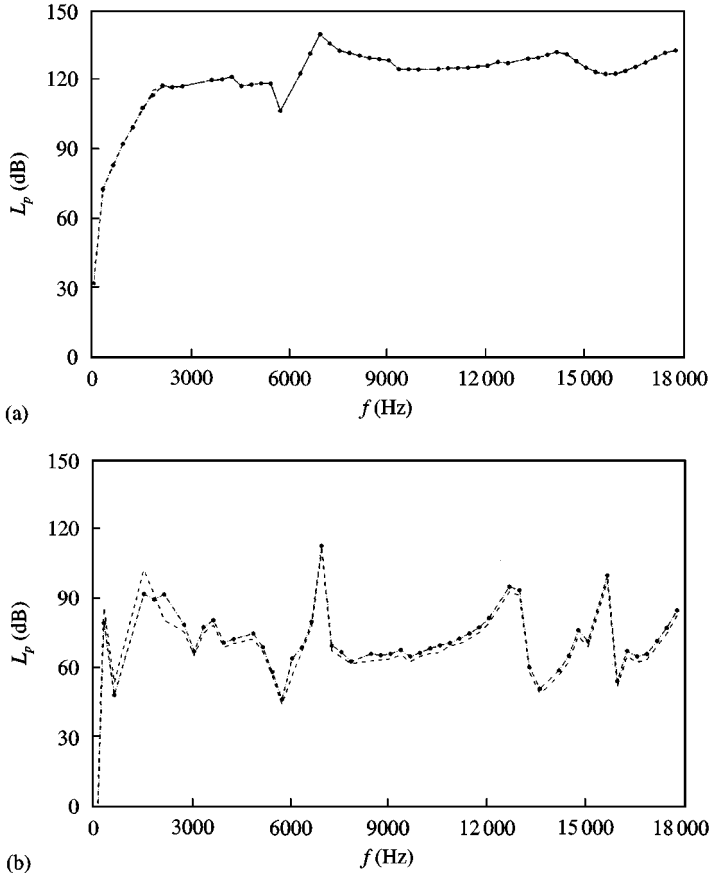

Figure 7. Similar to Figure 6, but the shells are filled with water and are immersed in water (a) and (b). ----, metal fibre; —●—, glass wool.

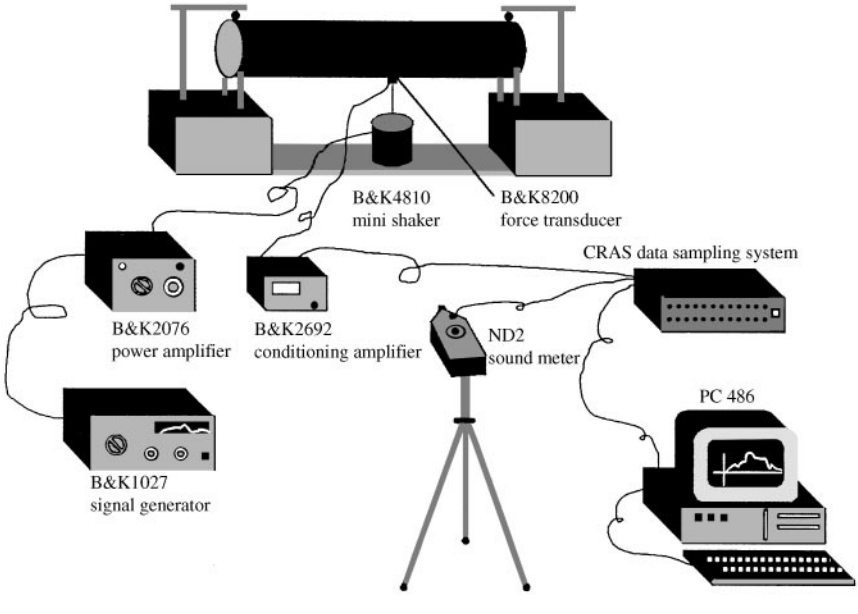

Figure 8. Sketch of the measurement system.

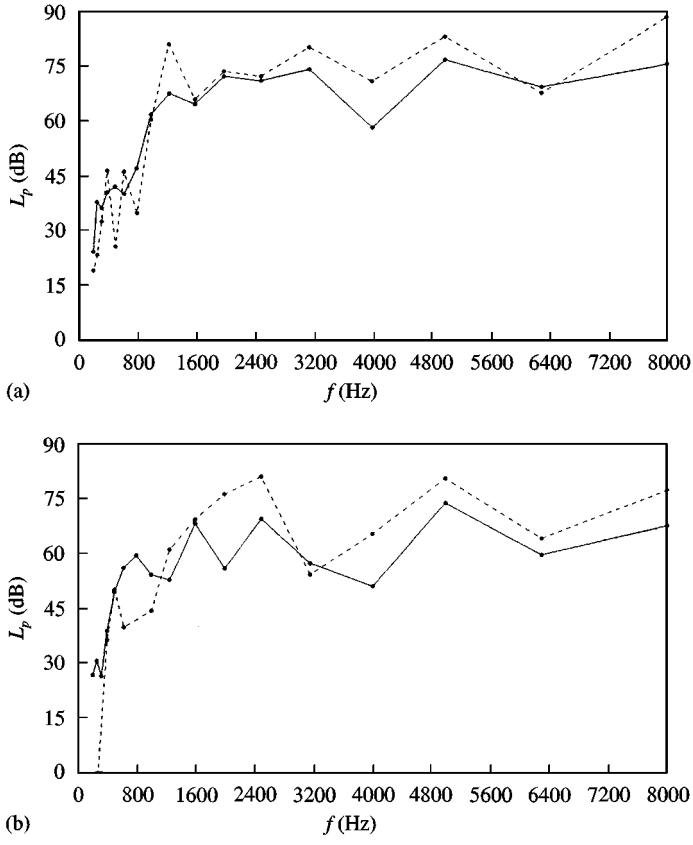

Figure 9. Far field sound radiation spectra of the experimental sandwich shell for the case of being filled with air and immersed in air. (a) External excitation only; (b) internal excitation only; —●—, experimental results; - - ● - -, theoretical results.

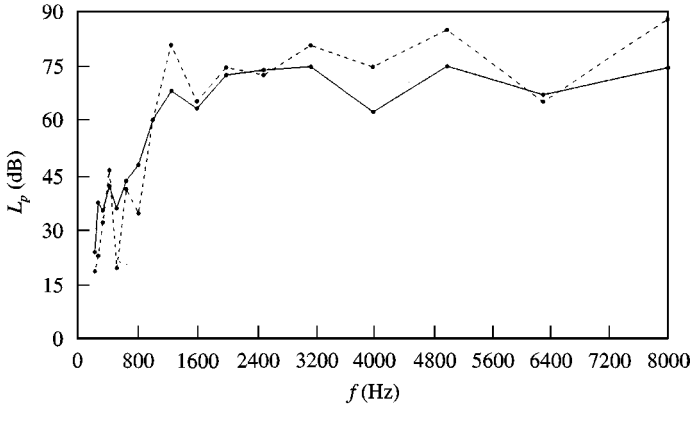

Figure 10. Far field sound radiation spectra of the experimental sandwich shell for the case of being filled with water and immersed in air, and under the external excitation only; —●—, experimental results; - - ● - -, theoretical results.

Finally, good correlation is obtained between the far field sound pressures measured on a finite fluid-filled/submerged cylindrical sandwich shell under a radial external point load and the theoretical model predictions. However, some discrepancies occurred in the comparisons. Further work is still required to make the theoretical model a practical design tool.

REFERENCES

1. M. L. MUNJAL 1997 *Noise Control Engineering Journal* **45**, 113–118. Acoustic analysis and parametric studies of lagged pipes.
2. E. A. SKELTON and J. H. JAMES 1993 *Journal of Sound and Vibration* **161**, 251–264. Acoustics of an anisotropic layered cylinder.
3. P. J. T. FILIPPI and D. HABAULT 1989 *Journal of Sound and Vibration* **131**, 13–23. Sound radiation by a baffled cylindrical shell. part 1: A numerical technique based on boundary integral equations.
4. D. HABAULT and P. J. T. FILIPPI 1989 *Journal of Sound and Vibration* **131**, 25–36. Sound radiation by a baffled cylindrical shell. part 2: A numerical technique based on boundary integral equations.
5. P. R. STEPHANISHEN 1982 *Journal of the Acoustical Society of America* **71**, 813–823. Modal coupling in the vibration of fluid-loaded cylindrical shells.
6. B. LAULAGNET and J. L. GUYADER 1994 *Journal of the Acoustical Society of America* **96**, 277–286. Sound radiation from finite cylindrical coated shells, by means of asymptotic expansion of three dimension equations for coating.
7. R. PANNETON, A. BERRY and F. LAVILLE 1995 *Journal of the Acoustical Society of America* **98**, 2165–2172. Vibration and sound radiation of a cylindrical shell under a circumferentially moving load.
8. C. J. WU, H. L. CHEN and X. Q. HUANG 1999 *Journal of Sound and Vibration* **225**, 79–94. Vibroacoustic analysis of a fluid-loaded cylindrical shell excited by a rotating load.
9. M. C. JUNGER and D. FEIT 1986 *Sound, Structures and Their Interaction*. Cambridge, MA: MIT Press, second edition.
10. C. J. WU, X. Q. HUANG and H. L. CHEN 199 *Proceedings of International Conference on Advanced Manufacturing Technology*, 1089–1092. Sound radiation from a baffled fluid-filled/submerged cylindrical shell.
11. C. J. WU 1999 *Ph.D. Thesis, Xi'an Jiaotong University*. Theoretical modeling and prediction on multilayer fluid-structure coupling for cylindrical shell.
12. J. D. ACHENBACH and J. QU 1986 *Journal of Sound and Vibration* **105**, 185–198. Resonant vibrations of a submerged beam.

APPENDIX A: EXPRESSION OF $p(R, \theta, \psi)$ IN THE FAR FIELD

Let (r_o, φ, z) and (R, θ, ψ) be the respective co-ordinates of the points M and N, then the sound pressures $p(r_o, \varphi, z)$ and $p(R, \theta, \psi)$ satisfy the following boundary integral equation [9]:

$$p(R, \theta, \psi) = \int_s \left[p(r_o, \varphi, z) \frac{\partial g(N|M)}{\partial r} - \frac{\partial p(r_o, \varphi, z)}{\partial r} g(N|M) \right] \mathrm{d}S. \tag{A1}$$

Here the function $g(N|M)$ is given by

$$g(N|M) = \frac{e^{\mathrm{j}k_o \| N - M \|}}{4\pi \| N - M \|}, \tag{A2}$$

where $\| N - M \|$ is the distance between N and M. For the case of far field, one can write (Achenbach and Qu [12])

$$\| N - M \| \approx R - [r_o \sin\theta \cos(\psi - \varphi) + z \cos\theta]. \tag{A3}$$

Inserting equation (A3) into equation (A2), the result is

$$g(N|M) \approx \frac{\mathrm{e}^{\mathrm{j}k_o\{R - [r_o \sin\theta\cos(\psi - \varphi) + z\cos\theta]\}}}{4\pi R}. \tag{A4}$$

In equation (A1), $\partial p(r_o, \varphi, z)/\partial r$ is given by (cf. references [2–9])

$$\frac{\partial p(r_o, \varphi, z)}{\partial r} = \mathrm{j}\omega\rho_0 \dot{u}_r(r_o, \varphi, z). \tag{A5}$$

Also, the expression of (A5) in the wave-number domain is (Skelton and James [2])

$$\tilde{p}_n(r_o, \zeta) = \mathrm{j}\omega\rho_0 \frac{\mathrm{H}_n(\gamma_0 r_o)}{\gamma_0 \cdot \mathrm{H}_n'(\gamma_0 r_o)} \tilde{\dot{u}}_{r,n}(r_o, \zeta). \tag{A6}$$

Let us consider equation (A1) consisting of two parts, p_1 and p_2, then we can write

$$p_1 = -\int_s \frac{\partial p}{\partial r}(r_o, \varphi, z) g(N|M)\,\mathrm{d}S, \quad p_2 = \int_s p(r_o, \varphi, z) \frac{\partial g(N|M)}{\partial r}\,\mathrm{d}S. \tag{A7a, b}$$

By combining equations (A4) and (A5) with equation (A7a), one can write

$$\begin{aligned} p_1 &= -\frac{\mathrm{e}^{\mathrm{j}k_o R}}{4\pi R}\mathrm{j}\omega\rho_0 r_o \int_0^{2\pi}\int_{-\infty}^{+\infty} \dot{u}_r(r_o, \varphi, z)\,\mathrm{e}^{-\mathrm{j}k_o r_o \sin\theta\cos(\psi - \varphi)} \cdot \mathrm{e}^{-\mathrm{j}k_o z\cos\theta}\,\mathrm{d}z\,\mathrm{d}\varphi \\ &= -\frac{\mathrm{e}^{\mathrm{j}k_o R}}{4\pi R}\mathrm{j}\omega\rho_0 r_o \sum_{n=-\infty}^{+\infty}\int_0^{2\pi}\left(\int_{-\infty}^{+\infty} \dot{u}_{r,n}(r_o, z)\,\mathrm{e}^{-\mathrm{j}k_o z\cos\theta\,\mathrm{d}z}\right)\mathrm{e}^{\mathrm{j}n\varphi}\,\mathrm{e}^{-\mathrm{j}k_o r_o \sin\theta\cos(\psi - \varphi)}\,\mathrm{d}\varphi \\ &= -\frac{\mathrm{e}^{\mathrm{j}k_o R}}{4\pi R}\mathrm{j}\omega\rho_0 r_o \sum_{n=-\infty}^{+\infty}\int_0^{2\pi} \tilde{\dot{u}}_{r,n}(r_o, k_o\cos\theta)\,\mathrm{e}^{-\mathrm{j}n\varphi}\,\mathrm{e}^{-\mathrm{j}k_o r_o \sin\theta\cos(\psi - \varphi)}\,\mathrm{d}\varphi. \end{aligned} \tag{A8}$$

By using the following relations [4]:

$$\mathrm{e}^{\mathrm{j}n\psi}\int_0^{2\pi} \mathrm{e}^{\mathrm{j}n(\varphi - \psi)} \cdot \mathrm{e}^{-\mathrm{j}k_o r_o \sin\theta\cos(\varphi - \psi)}\,\mathrm{d}(\varphi - \psi) = 2\pi \mathrm{J}_n(k_o r_o \sin\theta)\,\mathrm{e}^{\mathrm{j}n(\psi - \pi/2)} \tag{A9}$$

and

$$\cos(\varphi - \psi) = \cos(\psi - \varphi), \quad \mathrm{d}\varphi = \mathrm{d}(\varphi - \psi), \tag{A10a, b}$$

equation (A8) can be simplified as

$$p_1 = -\frac{\mathrm{e}^{\mathrm{j}k_o R}}{4\pi R} 2\pi\mathrm{j}\omega\rho_o r_o \sum_{n=-\infty}^{+\infty} \tilde{\dot{u}}_{r,n}(r_o, k_o\cos\theta)\,\mathrm{J}_n(k_o r_o \sin\theta)\,\mathrm{e}^{\mathrm{j}n(\psi - \pi/2)}. \tag{A11}$$

Similarly, inserting equation (A4) into equation (A7b), one can write

$$\begin{aligned} p_2 &= \frac{\mathrm{e}^{\mathrm{j}k_o R}}{4\pi R} r_o \int_0^{2\pi}\int_{-\infty}^{+\infty} p(r_o, \varphi, z)\,\mathrm{e}^{-\mathrm{j}k_o r_o \sin\theta\cos(\psi - \varphi)}[-\mathrm{j}k_o \sin\theta\cos(\psi - \varphi)]\,\mathrm{e}^{-\mathrm{j}k_o z\cos\theta}\,\mathrm{d}z\,\mathrm{d}\varphi \\ &= \frac{\mathrm{e}^{\mathrm{j}k_o R}}{4\pi R} r_o \sum_{n=-\infty}^{+\infty}\int_0^{2\pi}\left(\int_{-\infty}^{+\infty} p_n(r_o, z)\,\mathrm{e}^{-\mathrm{j}k_o z\cos\theta}\,\mathrm{d}z\right)\mathrm{e}^{\mathrm{j}n\varphi}\,\mathrm{e}^{-\mathrm{j}k_o r_o \sin\theta\cos(\psi - \varphi)} \\ &\quad \times[-\mathrm{j}k_o \sin\theta\cos(\psi - \varphi)]\,\mathrm{d}\varphi \\ &= \frac{\mathrm{e}^{\mathrm{j}k_o R}}{4\pi R} r_o \sum_{n=-\infty}^{+\infty}\int_0^{2\pi} \tilde{p}_n(r_o, k_o\cos\theta)\,\mathrm{e}^{\mathrm{j}n\varphi}\,\mathrm{e}^{-\mathrm{j}k_o r_o \sin\theta\cos(\psi - \varphi)}[-\mathrm{j}k_o \sin\theta\cos(\psi - \varphi)]\,\mathrm{d}\varphi. \end{aligned} \tag{A12}$$

By using the following relation (the derivation of both sides of equation (A9) with respect to r_o):

$$e^{jn\psi}\int_0^{2\pi} e^{jn(\varphi-\psi)}\, e^{-jk_o r_o \sin\theta\cos(\varphi-\psi)}\,[-jk_o\sin\theta\cos(\varphi-\psi)]\,d(\varphi-\psi)$$

$$= 2\pi k_o \sin\theta J_n'(k_o r_o\sin\theta)\, e^{jn(\psi-\pi/2)}, \tag{A13}$$

one can write

$$p_2 = \frac{e^{jk_o R}}{4\pi R}\, 2\pi r_o k_o \sin\theta \sum_{n=-\infty}^{+\infty} \tilde{p}_n(r_o, k_o\cos\theta)\, J_n'(k_o r_o\sin\theta)\, e^{jn(\psi-\pi/2)}. \tag{A14}$$

Substituting equation (A6) into equation (A14), the result is

$$p_2 = \frac{e^{jk_o R}}{4\pi R}\, 2\pi r_o j\omega\rho_o \sum_{n=-\infty}^{+\infty} \tilde{u}_{r,n}(r_o, k_o\cos\theta)\frac{H_n(k_o r_o\sin\theta)}{H_n'(k_o r_o\sin\theta)}\, J_n'(k_o r_o\sin\theta)\, e^{jn(\psi-\pi/2)}. \tag{A15}$$

While combining equation (A11) with equation (A15), one can easily obtain the expression of $p(R, \theta, \psi)$ as follows:

$$p(R,\theta,\psi) = p_1 + p_2$$

$$= \frac{e^{jk_o R}}{4\pi R}\, 2\pi r_o j\omega\rho_o \sum_{n=-\infty}^{+\infty}\left[J_n(k_o, r_o\sin\theta) - \frac{H_n(k_o r_o\sin\theta)}{H_n'(k_o r_o\sin\theta)}\, J_n'(k_o r_o\sin\theta)\right]$$

$$\times \tilde{u}_{r,n}(r_o, k_o\cos\theta)\, e^{jn(\psi-\pi/2)}$$

$$= \frac{e^{jk_o R}}{\pi R}\frac{\omega\rho_o}{k_o\sin\theta}\sum_{n=-\infty}^{+\infty}\frac{\tilde{u}_{r,n}(r_o, k_o\cos\theta)}{H_n'(k_o r_o\sin\theta)}\, e^{jn(\psi-\pi/2)}, \tag{A16}$$

where the following relation (cf. reference [9]) is used:

$$J_n(x) - \frac{H_n(x)}{H_n'(x)}J_n'(x) = \frac{j[J_n(x)Y_n'(x) - Y_n(x)J_n'(x)]}{H_n'(x)} = \frac{j\cdot 2/\pi x}{H_n'(x)}. \tag{A17}$$

APPENDIX B: NOMENCLATURE

a_1, a_2	neutral radius of the inner layer, the outer layer respectively
c_i	sound speed in the interior fluid
c_o	sound speed in the exterior fluid
c_f	sound speed of the fluid (air) entrapped in the pores of the porous material
E_1, E_2	Young's modulus of the inner layer, outer layer respectively
f	frequency
F_0	amplitude of the exciting force
$\tilde{F}_{r,n}$	spectral radial exciting force
$g(\ )$	free-space Green's function, defined in equation (A2)
h_1, h_2	thickness of the inner layer, outer layer respectively
$H_n(\ )$	the nth order Hankel function
$H_n'(\ )$	derivative of the nth order Hankel function with respect to its argument
$J_n(\ )$	the nth order Bessel function
$J_n'(\ )$	derivative of the nth order Bessel function with respect to its argument
k_i	sound wave number in the interior fluid, $= \omega/c_i$
k_o	sound wave number in the exterior fluid, $= \omega/c_o$

k_m complex wave number of the porous material (metal fibre), defined in equation (16)
k_f sound wave number of the fluid (air) entrapped in the pores of porous material, $= \omega/c_f$
L semi-length of the shell
L_p sound pressure level, defined in equation (23)
$\tilde{p}_n$ spectral sound pressure acting on fluid–structure surface
r_1, r_o external radius of inner layer, outer layer respectively
r_1, r_2 internal radius of inner layer, outer layer respectively
S outer surface of the shell
$\tilde{S}^+_{r,n}$, $\tilde{S}^+_{z,n}$, $\tilde{S}^+_{\varphi,n}$ radial, axial, and circumferential components of spectral boundary source vectors at $z = L$ of shell
$\tilde{S}^-_{r,n}$, $\tilde{S}^-_{z,n}$, $\tilde{S}^-_{\varphi,n}$ radial, axial, and circumferential components of spectral boundary source vectors at $z = -L$ of shell
$[\mathbf{T}_m]$ transfer matrix of the porous material layer, defined in equation (11)
$\tilde{u}_{r,n}$, $\tilde{u}_{z,n}$, $\tilde{u}_{\varphi,n}$ radial, axial, and circumferential components of spectral displacement vectors of the inner layer or outer layer
$\tilde{\dot{u}}_{r,n}$ spectral radial velocity of the surface of the inner or outer layer
$\tilde{X}_n$ spectral variable defined in equation (4)
Y_f characteristic impedance of the fluid (air) entrapped in porous material, $= \rho_f c_f$
Y_m complex characteristic impedance of porous material (metal fibre), defined in equation (15)
$\mathrm{Y}_n(\ )$ the nth order Neumann function
$\mathrm{Y}'_n(\ )$ derivative of the nth order Neumann function with respect to its argument
$\tilde{Z}_{1,n}$ spectral radial mechanical impedance of the inner layer, defined in equation (8)
$\tilde{Z}_{2,n}$ spectral radial mechanical impedance of the outer layer
$\tilde{Z}_{i,n}$ spectral radiation impedance in the interior fluid, defined in equation (19)
$\tilde{Z}_{o,n}$ spectral radiation impedance in the exterior fluid, defined in equation (20)
δ Dirac Delta function
ρ_i, ρ_o density of the interior fluid, exterior fluid respectively
ρ_1, ρ_2 density of the inner layer, outer layer respectively
ρ_m density of the porous material
γ_i radial wave number in the interior fluid, $= \sqrt{k_i^2 - \zeta^2}$
γ_o radial wave number in the exterior fluid, $= \sqrt{k_o^2 - \zeta^2}$
γ_m radial wave number of the porous material, $= \sqrt{k_m^2 - \zeta^2}$
ν_1, ν_2 Poisson's ratio of the inner layer, outer layer respectively
ω circular frequency, $= 2\pi f$
ζ axial wave number
$[\tilde{\Gamma}_n]$ spectral matrix of classical Donnell's differential operator
$\tilde{\Gamma}^1_{n3}$, $\tilde{\Gamma}^2_{n3}$, $\tilde{\Gamma}^3_{n3}$ three elements of the third row of the matrix $[\tilde{\Gamma}_n]$